Neighboring Aliphatic/Aromatic Side Chain Interactions between Residues 9 and 10 in Gramicidin Channels†

Roger E. Koeppe II,*,‡ Jesse Hatchett,‡ Anthony R. Jude,‡ Lyndon L. Providence,§ Olaf S. Andersen,§ and Denise V. Greathouse‡

Department of Chemistry and Biochemistry, University of Arkansas, Fayetteville, Arkansas 72701, and Department of Physiology and Biophysics, Weill Medical College of Cornell University, New York, New York 10021

Received September 2, 1999; Revised Manuscript Received December 3, 1999

ABSTRACT: The interactions between an aliphatic or phenyl side chain and an indole ring in a phospholipid environment were investigated by synthesizing and characterizing gramicidins in which Trp[9] was ring-labeled and D-Leu[10] was replaced by D-Val, D-Ala, or D-Phe. All three analogues form conducting channels, with conductances that are lower than that of gramicidin A (gA) channels. The channel lifetimes vary by less than 50% from that of gA channels. Circular dichroism spectra and size-exclusion chromatography show that the conformation of each analogue in dimyristoylphosphatidylcholine (DMPC) vesicles is similar to the right-handed $\beta^{6.3}$-helical conformation that is observed for gA. ^{2}H NMR spectra of oriented samples in DMPC show large changes for the Trp[9] ring when residue 10 is modified, suggesting a steric interaction between D-Leu[10] and Trp[9], in agreement with previous acylation studies (R. E. Koeppe II et al. (1995) *Biochemistry 34*, 9299−9307). The outer quadrupolar splitting for Trp[9] is unchanged with D-Phe[10], at ∼153 kHz, but increases by ∼25 kHz with D-Val[10] and decreases by ∼10 kHz with D-Ala[10]. With D-Ala[10] or D-Val[10], the outer resonance splits into two in a temperature-dependent manner. The NMR spectra indicate that the side chain torsion angles $\chi1$ and $\chi2$ for Trp[9] change when residue 10 is substituted. The changes in $\chi1$ are small, in all cases less than 10°, as is $\Delta\chi2$ when D-Ala[10] is introduced, but with D-Val[10] and D-Phe[10] $\Delta\chi2$ is at least 25°. We conclude that D-Leu[10] helps to stabilize an optimal orientation of Trp[9] in gA channels in lipid bilayers and that changes in Trp orientation alter channel conductance and lifetime without affecting the basic channel fold.

Site-directed mutagenesis often is used to identify and verify residues at the active sites of proteins. For example, mutations of critical catalytic residues may knock out enzymatic activity. The positions of these critical residues, however, are maintained by a scaffolding provided by neighboring residues, which themselves have no direct catalytic function. Mutations of such "noncritical" residues also may have large effects on function. Despite their importance, it may be difficult to decipher the consequences of mutations of such neighboring residues because they have more subtle, indirect, or secondary influences on catalytic activity. We have examined this question in the case of gramicidin A (gA) channels, which are formed by two $\beta^{6.3}$-helical subunits with the sequences HCO-L-Val[1]-Gly[2]-L-Ala[3]-D-Leu[4]-L-Ala[5]-D-Val[6]-L-Val[7]-D-Val[8]-*L-Trp[9]-D-Leu[10]*-L-Trp[11]-D-Leu[12]-L-Trp[13]-D-Leu[14]-L-Trp[15]-$NHCH_2CH_2OH$ (*1*). (The two italicized residues are the focus of the present investigation.)

In gramicidin channels, the four tryptophans are crucial for channel folding and assembly (*2*−*7*), ion transport (*8*−*11*), and channel stability (*12*). The leucine spacers between the tryptophans play an important, but only recently recognized, secondary role for ion permeability and channel lifetime. Replacement of all three leucines with other similar aliphatic side chains produces distinct changes in channel properties and increases the proportion of molecules that fold into nonchannel states in a bilayer environment (*13*).

In order better to understand the basis for these effects of the leucine residues, we decided to focus on the L-Trp[9]-D-Leu[10] region of the sequence.[2] Generally, the Trp and D-Leu residues that span positions 9−15 are situated at the membrane/water interface in the folded gA[1] channel in a lipid bilayer and form the mouth of the channel (*14*, *15*). The preference of the tryptophans for the interface (as opposed to either the membrane interior or the aqueous phase) drives channel folding and bilayer insertion (*3*−*6*, *16*, *17*). In

† This work was supported in part by grants GM34968 and GM21342 from the NIH.

* To whom correspondence should be addressed at the University of Arkansas. Phone: 501-575-4976. Fax: 501-575-4049. E-mail: rk2@uafsysb.uark.edu.

‡ University of Arkansas.

§ Weill Medical College of Cornell University.

[1] Abbreviations: gA, gramicidin A.; CD, circular dichroism; DMPC, dimyristoylphosphatidylcholine; DPhPC, diphytanoylphosphatidylcholine; DS, double-stranded; LH, left-handed; NMR, nuclear magnetic resonance; NOE, nuclear Overhauser enhancement; PDB, Protein Data Bank; QCC, quadrupolar coupling constant; RH, right-handed; SDS, sodium dodecyl sulfate; SEC, size-exclusion chromatography; SS, single-stranded;.

[2] When triple substitutions are introduced by simultaneously replacing the D-leucines at positions 10, 12, and 14 in gA, the resulting gramicidins exhibit at least two conformations in DMPC vesicles (*13*). In the present work, therefore, we chose to replace only one of the D-leucines in an attempt to achieve a single conformation that could be characterized by NMR.

10.1021/bi9920679 CCC: $19.00
Published on Web 02/12/2000

addition, the Trp[9]-D-Leu[10] region may exhibit some flexibility, as there is disagreement about the orientation of Trp[9] (*18, 19*).

Among the leucines, D-Leu[10] is in a particularly special environment in which it is highly shielded by a Trp indole ring (*19*). In SDS micelles (*14, 20*), it is the indole ring of Trp[9] that shields D-Leu[10], but some reports have suggested that Trp[9] may adopt a different conformation in DMPC membranes (*15, 18*). Solid-state ^{2}H NMR spectra from oriented samples of ring-labeled-Trp[9]-gA have not resolved the question because the spectra are geometrically consistent with four different ring orientations that all would give similar spectra (*21, 22*). The issue is complicated further because the resonances in such spectra can be assigned to the ring in several different ways (*18*).

It thus becomes important to clarify further the orientation and spectral assignment for Trp[9] and to characterize the functional roles of D-Leu[10]. To this end we investigated gramicidin analogues in which Trp[9] is ring-labeled with deuterium and D-Leu[10] is replaced by D-Ala, D-Val, or D-Phe. The functional results support the roles of D-Leu[10] that were inferred previously from triple substitutions[2] of D-Leu[10,12,14] in gA (*13*). The structural results allow us to suggest a preferred ^{2}H NMR spectral assignment for Trp[9] and a close proximity of the side chains of Trp[9] and D-Leu[10] when gA is in its channel conformation. The results also show quantitatively the magnitude of the changes in the average side-chain $\chi1$ and $\chi2$ angles of Trp[9] when D-Leu[10] successively is changed to D-Ala, D-Val, and D-Phe. These changes show that the conformation of Trp[9] is determined in part by packing interactions between the aliphatic and aromatic side chains.

MATERIALS AND METHODS

Labeled, substituted gramicidins were synthesized as described by Greathouse et al. (*23*).

CD Spectroscopy and SEC. Samples for CD spectroscopy and SEC in DMPC were prepared as described previously (*24*) using 0.05 μmol of gA analogue plus 1.5 μmol of DMPC (1:30 gramicidin:lipid ratio) in a final volume of 500 μL of H_2O. Briefly, dry gramicidin/lipid films were prepared by evaporating all traces of solvent from methanol/chloroform solutions, resuspending in N_2-flushed H_2O, and sonicating at 55 °C to produce small vesicles. CD spectra were recorded at 22−24 °C using a JASCO J-710 circular dichroism spectrometer with a 0.1 cm path length cell, 1.0 nm bandwidth, 0.2 nm step resolution, and 20 or 50 nm/min scan speed. SEC was performed at room temperature (*7*) using an Ultrastyragel 1000 Å column (Waters, Inc., Milford, MA) with a tetrahydrofuran mobile phase at a flow rate of 1.0 mL/min.

Electrophysiology. Single-channel measurements were done in planar bilayers formed from DPhPC in *n*-decane (2−3% w/v) at 25 ± 1 °C, using the bilayer punch method (*25*). Sample preparation was as described by Mattice et al. (*26*). Gramicidins were added in amounts necessary to produce ~1 channel event per second.

^{2}H NMR Spectroscopy. Oriented samples, with 1:10 gramicidin:DMPC and 40% hydration, for ^{2}H NMR spectroscopy were prepared and spectra recorded with the normal to the glass plates either parallel ($\beta = 0°$) or perpendicular ($\beta = 90°$) to the magnetic field, H_o, as described previously (*27*). For the analysis of ^{2}H NMR data, a modification of an earlier procedure (*22*) was used. Deuterium quadrupolar splittings relate to orientation angles for the C−^{2}H bonds of the labeled indole ring according to the equation (*28*)

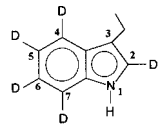

FIGURE 1: Structure and numbering of a deuterated (d_5) indole ring of tryptophan.

$$\Delta\nu_q = (3/2)(e^2qQ/h)(^1/_2[3\cos^2\Theta - 1])(^1/_2[3\cos^2\beta - 1]) \quad (1)$$

in which e^2qQ/h is the C−^{2}H quadrupolar coupling constant, Θ is the angle between a C−^{2}H bond and the axis of rapid whole-molecule reorientation (the channel axis, which is normal to the glass plates and the membranes), and β is the angle between the membrane normal and the magnetic field, H_o. To match Θ values with $\Delta\nu_q$ values, the Trp[9] side chain—attached to one of several particular backbone models (see below)—was rotated through 0.5° intervals in $\chi1$ and $\chi2$, as described in ref *22*. For each ring orientation, $\Delta\nu_q$ values were calculated for the ring C−^{2}H bonds, according to eq 1, and compared to the spectral quadrupolar splittings. With the provision that each ring deuteron was assigned to a different value of $\Delta\nu_q$ (see ref *22*), the goodness of fit of a particular ring orientation to the data was expressed as the root-mean-squared deviation between the $\Delta\nu_q$ values calculated from the model and those observed in the NMR spectra:

$$\%\ \text{rmsd} = 100\%([\Sigma\{(\Delta\nu_{qo} - \Delta\nu_{qc})/\Delta\nu_{qo}\}^2]/N)^{1/2} \quad (2)$$

where N is the number of quadrupolar splittings being considered, and $\Delta\nu_{qo}$ and $\Delta\nu_{qc}$ are the spectrally observed and model calculated values of $\Delta\nu_q$, respectively. (For statistical reasons, the average of the C4 and C7 $\Delta\nu_q$'s was included only once in the sum.)

In the fitting procedure, the static quadrupolar coupling constant, e^2qQ/h, was expressed as m(180 kHz), where 180 kHz is a characteristic value for ring deuterons (*29*) and m is an adjustable parameter between 0.0 and 1.0 to reflect motional averaging (*22, 28*). Though m is sometimes found to vary slightly for different ring positions (*18*), we fit a single value of m for each Trp[9] ring. Then, solely for the purpose of estimating the uncertainty in m at the end of a refinement, we determined what site-to-site variation in m would be necessary to optimize each fit of the $\Delta\nu_q$ values to the ring geometry. We report the results for each analogue as $m \pm$ this uncertainty.

The process of deducing an indole ring orientation from a set of quadrupolar splittings measured from an NMR spectrum requires an assignment of the magnitude and sign of each $\Delta\nu_q$ value to a particular C−^{2}H bond in the ring (*22*). The spectrum of [d_5-Trp[9]]gA can be assigned on the basis of four different schemes (*18*) that differ in the assignment of the C4−^{2}H and C7−^{2}H bonds (Figure 1), which are essentially parallel to each other.[3] Remarkably (and fortunately), each ring assignment scheme gives a similar

set of choices for the Trp[9] ring orientation (*18*). We tested several possible assignments for the C4/C7 deuterons.

Difference Analysis. Regardless of the spectral assignments of the ring (*18*), the ^{2}H NMR method yields four comparable solutions for a given indole ring orientation, which are geometrically equivalent with respect to H_o (*21*, *22*). To assess the extent of the *change* in the Trp[9] average orientation when D-Leu[10] was substituted, we used all four possible solutions for a difference analysis between gA and each analogue. From the four sets of solutions, minimal and average values of $\Delta\chi1$ and $\Delta\chi2$ were calculated. This approach renders the difference comparisons independent of any uncertainties regarding the choice of particular local starting values of $\chi1$ and $\chi2$ for Trp[9] (*18*).

Choice of Backbone. It is desirable that a difference analysis of the change in Trp[9] average orientation, when residue 10 is substituted, be independent of the particular backbone model that is used. Models of the backbone of the gA channel are available from solution NMR in SDS and solid-state NMR in DMPC, and both of these backbone models were tested. For the solution NMR model, we used a backbone derived from the coordinates of Arseniev et al. (*14*), as refined in ref *28*. For the solid-state NMR model, we used coordinates from the Protein Data Bank (PDB), entry 1MAG (*30*). Both models gave the same results concerning $\Delta\chi1$ and $\Delta\chi2$ for Trp[9].

Planar Indole Rings. Steps were taken to ensure the planarity of the indole rings. Theory and experiment agree that the three lowest electronic states of indole are planar with C_s symmetry; this statement is supported fully by X-ray crystallography (*31*), including electron density analysis (*32*), microwave spectroscopy (*33*), and ab initio calculations (*34*, *35*). The original Arseniev (*14*) coordinates represented planar rings, but we found that the program Discover (Biosym-MSI, San Diego, CA) introduced significant distortions from ring planarity during the refinement described in ref *28*. Also the PDB model 1MAG (version of 11-Jan-97, refined using CHARMM (*30*)) has distinctly nonplanar indole rings. On the basis of the experimental and theoretical verification of the C_s symmetry, one must assume that the nonplanarity is an artifact of the refinement methods. To correct this problem, we used the program InsightII (Biosym-MSI) to remove the indole rings from the refined Arseniev and 1MAG models and replaced them with planar indole rings from the Biopolymer library of InsightII, prior to the determination of the best ($\chi1$, $\chi2$) fits to the NMR data.

RESULTS

Channel Properties. All three D-Leu[10]—replaced analogues form conducting channels in DPhPC membranes. This was anticipated because similar triple substitutions at positions 10, 12, and 14 had yielded gramicidins that formed transmembrane channels (*13*). Figure 2 summarizes the single-channel results. The channels formed by the D-Ala[10] and D-Val[10] analogues have conductances that are slightly lower than gA (in 1 M NaCl) and average channel lifetimes that are intermediate between those of gA and the corresponding triply substituted analogue with D-Ala or D-Val at positions 12 and 14 as well as position 10 (Table 1). Relative to gA, single substitutions of only D-Ala[10] or D-Val[10] yield about the same percentage reduction in cation conductance as do the triple substitutions of D-Ala[10,12,14] or D-Val[10,12,14]. (From Table 1, the reductions are ~15% for D-Val[10] and ~20% for D-Ala[10], with further reductions of only ~5% when additional substitutions are introduced at positions 12 and 14.) [D-Phe[10]]gA channels have ~50% of the conductance of gA channels and a comparable lifetime (Table 1).

Structural Information from CD Spectroscopy and SEC. All of the position-10 analogues of gA have a predominant SS RH conformation in DMPC membranes. This situation contrasts with the conformational mixtures that have been observed with the triply substituted position-10, -12, -14 analogues[2] (*13*). The positive ellipticity at 218 and 235 nm in the CD spectra of the position-10 analogues (Figure 3) is much more intense than in corresponding spectra for triply substituted analogues (*13*) and is strong evidence for a dominant SS RH conformation for each of the single-site analogues. While the negative minimum at 229 nm (especially Figure 3D) suggests a small fraction of double-stranded conformers (although much less than for any of the position-(10, 12, 14) analogues), the intensity of the negative peak nevertheless varies somewhat with particular details of sample preparation and "history," even for native gA (*36*−*38*).

The SEC chromatograms (Figure 4) provide further confirming evidence that the membrane-bound position-10 gA analogues are monomeric (~95% SS).[4] In each chromatogram, a major peak representing SS monomers is preceded by only a small shoulder (~0.5 min earlier) that represents a minor population of inert DS dimers (see also (*13*)). While the SEC results suggest even smaller amounts of DS conformers than may have been inferred from the CD spectra in Figure 3, the methods are in overall excellent agreement that the major conformation for each analogue is a functionally active SS channel that also gives rise to the sodium conductance events shown in Figure 2. On the basis of previous correlations between CD and NMR spectroscopy, one can conclude that this major conformation in each case is a RH $\beta^{6.3}$ channel. Even with native gA, a minor proportion of DS conformer(s) is evident in Figure 4, and the proportion increases only slightly with the substitutions at position 10. (In experiments such as those in Figure 4, the peak-to-peak separation is highly reproducible from chromatogram to chromatogram, even though the absolute retention times may vary up to 5% due to minor variations in temperature or flow rate).

Importantly, the presence of a single dominant (SS RH) conformation makes these analogues suitable for labeling and ^{2}H NMR spectroscopy using oriented samples, as one can be confident that the ^{2}H resonances will reflect the SS RH $\beta^{6.3}$ channel conformation and not some other inactive conformation. We therefore undertook the ^{2}H NMR analysis of the labeled Trp[9] ring as a function of the identity of the residue at position 10.

[3] Though parallel, the C4−^{2}H and C7−^{2}H bonds of an indole ring generally will give slightly different $\Delta\nu_q$'s, due to the closer proximity of the C7−^{2}H to the ring N−H, and to the small off-bond component of the spin interaction tensor (*22*).

[4] Because the membrane-bound gA channel dimer is held together by only 6 hydrogen bonds that link the monomers, the channel dissociates to monomers when injected into the tetrahydrofuran elution solvent that is used for SEC (*55*).

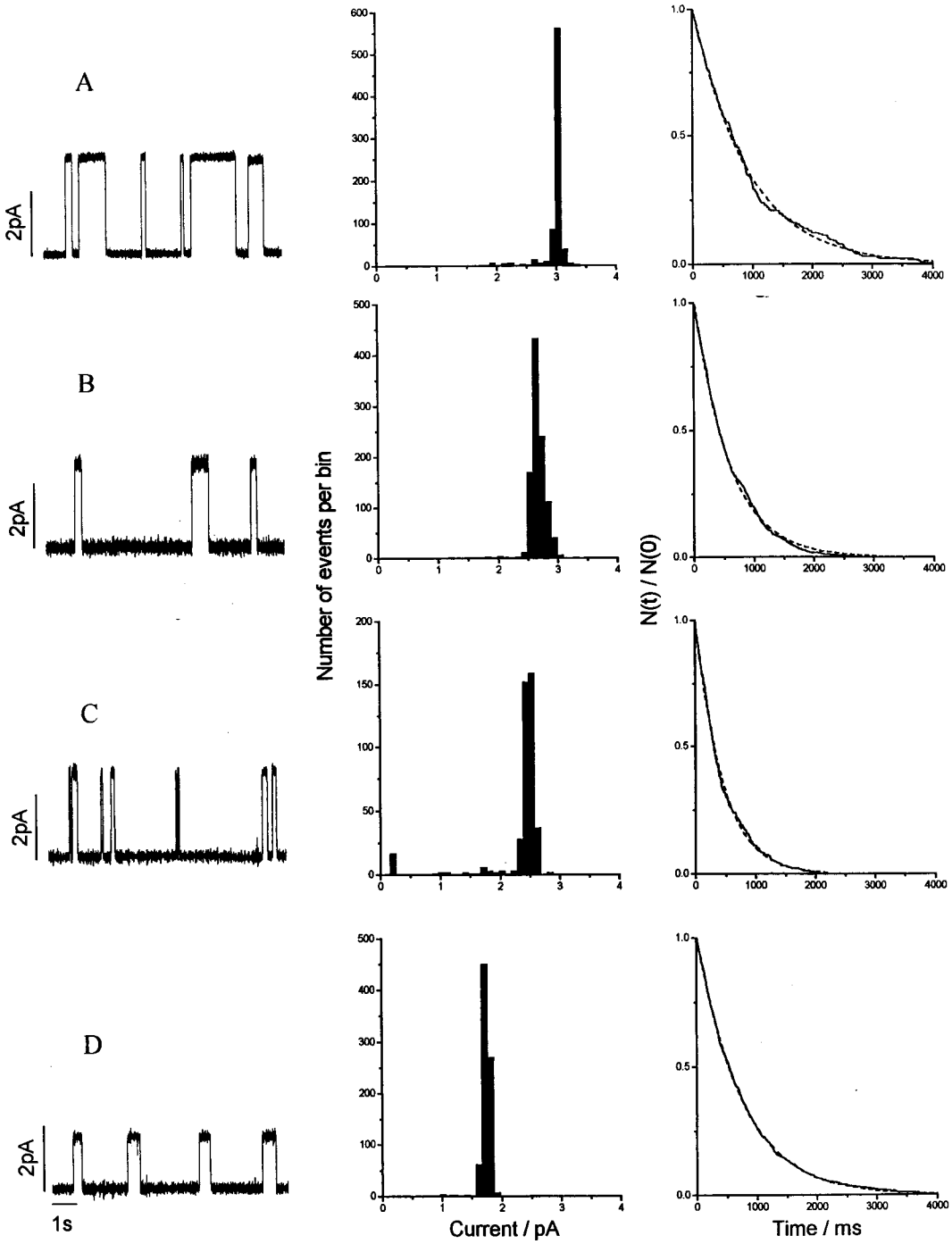

FIGURE 2: Single-channel current traces (left), conductance histograms (center), and duration distributions (right) for channels formed by (A) gA; (B) [D-Ala10]gA; (C) [D-Val10]gA; (D) [D-Phe10]gA. The single-channel conductances and average channel durations are summarized in Table 1. Calibration bars: 2 pA vertical, and 1 s horizontal. 1.0 M NaCl, 200 mV, 25 °C.

^{2}H NMR Spectroscopy. *Spectra.* Figure 5 shows the spectra from d_5-Trp^9 in oriented samples of gramicidin/DMPC with different residues at position 10. The spectrum of Trp^9 in gA (with D-Leu^{10}) shows four resonances, as reported previously (*18*, *22*). One of these resonances represents two deuterons, those at ring positions C4 and C7 (Figure 1).

From the spectra in Figure 5, it is evident that the d_5-Trp^9 ring quadrupolar splittings vary with the identity of residue 10. For [D-Ala^{10}]gA, the resonance positions are quite close to those in native gA, although the relative intensities change and several peaks twin; similar results have been observed also when this sample is oriented at $\beta = 90°$ (*39*). For [D-Val^{10}]gA, the outer peaks are twinned and their quadrupolar splitting is increased significantly to about 180 kHz. For [D-Val^{10}]gA and [D-Phe^{10}]gA, several resonances broaden and cluster together in the range of $\Delta\nu_q$ from about 65−85 kHz, so that the precise number of peaks is uncertain. This broadening and clustering may suggest increased conformational uncertainty and/or motion on an intermediate time scale. Similar results recently were reported for deuterated (ring-d_4)-5-F- and -6-F-Trp^9 in gA (*40*).

Trp^9 Ring Orientations and Spectral Assignments. A standard procedure (*22*) was used to rotate a planar indole ring at Trp^9 through all possible values of $\chi1$ and $\chi2$ in 0.5° increments. This procedure was then modified slightly to calculate quadrupolar splittings from the molecular geometry

Table 1: Single-Channel Conductances and Average Channel Durations for Position-10 and Position-10, -12, -14 Analogues of GA

single substitutions[a]	*g* (pS)	relative *g*	τ (ms)
D-Leu^{10} (native)	15.5	100%	890
D-Ala^{10}	12.5	81%	440
D-Val^{10}	13.3	86%	580
D-Phe^{10}	8.4	54%	750
triple substitutions[b]	***g* (pS)**	**relative *g***	**τ (ms)**
D-Leu^{10,12,14} (native)	47.2	100%	800
D-Ala^{10,12,14}	36.4	77%	100
D-Val^{10,12,14}	38.3	81%	400

[a] 1.0 M NaCl, 200 mV, 25 °C. [b] Data from ref 13, 1.0 M CsCl, 200 mV, 25 °C.

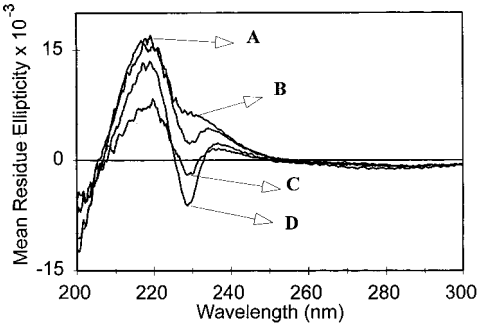

FIGURE 3: CD spectra of gramicidin analogues dispersed in aqueous DMPC (1:30, peptide:lipid): (A) gA; (B) [D-Ala10]gA; (C) [D-Val10]gA; (D) [D-Phe10]gA.

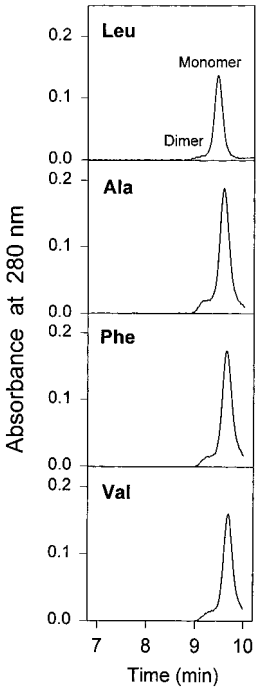

FIGURE 4: Size-exclusion chromatograms of gramicidin analogues dispersed in aqueous DMPC (1:30, peptide:lipid), and then injected into a tetrahydrofuran mobile phase. The identity of the D-residue at position 10 is indicated for gA (D-Leu), [D-Ala10]gA, [D-Val10]-gA, and [D-Phe10]gA. The positions at which the SS monomer and DS dimer conformations elute are indicated.

(instead of vice versa). The preferred values of $\chi1$ and $\chi2$ that emerge from such an analysis depend on the spectral assignments and the details of the backbone geometry, because $\chi1$ and $\chi2$ are coupled to the backbone. If the C4/C7 deuterons (Figure 1) can be assigned, then the other assignments will follow (*22*).

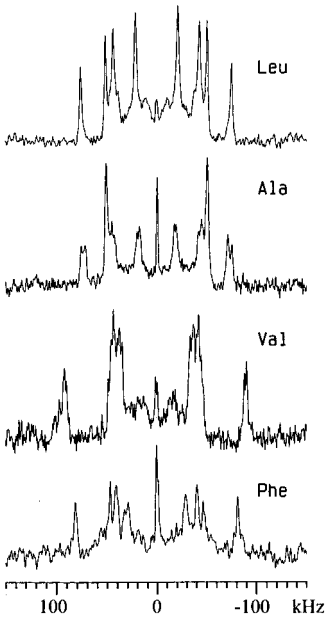

FIGURE 5: ^{2}H NMR spectra for 6 μmol of d_5-Trp9-labeled gramicidin oriented in 120 μmol of DMPC at ~40% (w/w) hydration, $\beta = 0°$ sample orientation, and temperature of 40 °C. The identity of residue 10 is indicated for (from top to bottom) gA, [D-Ala10]gA, [D-Val10]gA, and [D-Phe10]gA.

Table 2: Quadrupolar Interactions for Ring C$-^2$H Bonds and Side-chain Orientation of Trp^9 as Functions of Residue 10 Identity in gA[a]

	(residue 10) and $\Delta\nu$q in kHz			
Trp^9 ring position	(Leu)	(Ala)	(Val)	(Phe)
C2	−88	−90	−75	−64
C4, C7	153	143, 151	178, 181	155
C5	43	37	68	77
C6	−104	−102	−86	−87

other parameters	(Leu)	(Ala)	(Val)	(Phe)
Trp^9 $\Delta\chi1$	0.0°	1.8 ± 0.2°	7.7 ± 1.3°	3.6 ± 0.4°
Trp^9 $\Delta\chi2$	0.0°	3.3 ± 1.5°	36 ± 7°	27 ± 4°
ring QCC (kHz)	155 ± 2	155 ± 2	137 ± 3	131 ± 3
ring *m*	0.86 ± 0.01	0.86 ± 0.01	0.76 ± 0.02	0.73 ± 0.02

[a] The ring positions are identified and numbered in Figure 1. Values of $\Delta\nu_q$ are reported for the $\beta = 0°$ sample orientation; temperature 40 °C. $\Delta\chi1$ and $\Delta\chi2$ are expressed relative to ($\chi1$, $\chi2$) for gA of (197°, 86°) for an Arseniev backbone and (203°, 80°) for a Ketchem backbone. The parameter *m* is (QCC)/(180 kHz).

Four possible ways of assigning the C4/C7 deuterons have been reported (*18*). The twinning of the outermost peaks for d_5-Trp^9 in [D-Val^{10}]gA (Figure 5) has two possible explanations: either the C4/C7 deuterons should be assigned to the largest $\Delta\nu_q$, or the spectrum represents two slightly different ring orientations (or both features could be true). Our method indeed gave the best fit with the assignments listed in Table 2, i.e., when the C4/C7 deuterons in a flat Trp^9 ring were assigned to the largest quadrupolar splitting in the spectrum for each position-10 analogue. For [D-Val^{10}]gA and [D-Phe^{10}]-gA, we have been unable to fit the spectra with any other assignments. For [D-Ala^{10}]gA, the outermost peaks again are twinned, as are the peaks with $\Delta\nu_q$ near 37 kHz and 90 kHz.

The magnitudes and signs of the quadrupolar splittings for each of the gramicidins, according to our best fits, are summarized in Table 2. Although we have assigned resonances to the ring as shown in Table 2, the conclusions about $\Delta\chi1$ and $\Delta\chi2$ (below) are independent of the particular assignment scheme.

Backbone Dependence. To assess the backbone dependence of the $\chi1$ and $\chi2$ estimates for the planar Trp^9 ring in gA, [D-Ala^{10}]gA, [D-Val^{10}]gA, and [D-Phe^{10}]gA, we used backbones derived from both the Arseniev (*14*) two-dimensional NMR structure (*28*), and the solid-state NMR structure (1MAG in the Protein Data Bank (*30*)). The results of the calculations show that the ring orientations do not depend on the choice of backbone; in fact, the $\chi1$ and $\chi2$ torsions can function as a flexible swivel that adapts a particular ring orientation to a particular backbone geometry. The absolute $\chi1$ and $\chi2$ values therefore vary with subtle changes in the backbone, for example, from (197°, 86°) for an Arseniev backbone to (203°, 80°) for the same Trp^9 ring orientation on the 1MAG backbone from solid-state NMR. Importantly, however, the calculated *changes* in Trp^9 $\chi1$ and $\chi2$ ($\Delta\chi1$ and $\Delta\chi2$), as residue 10 is changed do not depend on the choice of backbone. We have obtained equivalent results using either the Arseniev or the Ketchem backbone.

Influence of Residue 10 on Trp^9 $\chi1$ and $\chi2$. For a given assignment of the ^{2}H NMR resonances to the Trp^9 ring (see above), four sets of ($\chi1$, $\chi2$) values provide comparable ring orientations with respect to the molecular long axis (and the magnetic field). The four sets therefore are mathematically nearly equivalent solutions for matching the molecular geometry to the ^{2}H NMR spectrum (*21*, *22*). Different authors have had individual reasons for selecting different unique members of the set of four possible ($\chi1$, $\chi2$) values[5] as "most probable" for Trp^9 (*18*, *19*, *27*).

To obtain results that would be independent of an initial choice of $\chi1$ and $\chi2$ for Trp^9, we used the $\Delta\nu_q$ data in Table 2 to calculate $\Delta\chi1$ and $\Delta\chi2$ for each position-10 analogue starting from each of the four conceivable initial ($\chi1$, $\chi2$) sets for Trp^9 in gA. The $\Delta\chi1$ and $\Delta\chi2$ values for each analogue at each of the four starting positions were then averaged. The results (and standard deviations within each set) are summarized in Table 2. Although $\chi1$ is only little affected by the position-10 substitutions, there are appreciable effects on $\chi2$. Also, a substitution of D-Val^{10} or D-Phe^{10} causes a larger $\Delta\chi2$ for Trp^9 than does the introduction of D-Ala^{10}. With D-Ala^{10}, the change in $\chi1$ is only about 1.5°, while $\Delta\chi2$ is about 3°, whereas the effects of a β-branched Val or Phe at position 10 are larger. With D-Phe^{10} and D-Val^{10}, the changes in $\chi1$ remain modest, ~3° and ~7°, respectively, but the $\Delta\chi2$'s are ~27° (±5°) for D-Phe^{10} and ~36° (±7°) for D-Val^{10}. The results show that the average orientation of Trp^9 depends on the identity of the residue at position 10. (If a position-10 substitution caused the Trp^9 ring to move to a different allowed region of conformational space, then the changes in $\chi1$ and $\chi2$ would be even larger. The $\Delta\chi$ values listed in Table 2 therefore are lower limits.)

Along with the changes in average orientation, the fits to the NMR results suggest that the dynamics of Trp^9 also are influenced by residue 10: the motion parameter *m* (see Methods) changes from 0.86 ± 0.01 in gA and [D-Ala^{10}]gA to 0.76 ± 0.02 and 0.73 ± 0.02 in [D-Val^{10}]gA and [D-Phe^{10}]-gA, respectively. (A decrease in *m* means that the side chain has increased mobility.) For comparison, deuterons on the backbone of gA are motionally averaged to about 0.92 of their maximum static QCC (*28*, *41*−*43*).) Taken together, the results for both average orientation and dynamics suggest that there are steric interactions between the side chains at positions 9 and 10 (see Discussion).

[5] In the computationally refined structure of gA in DMPC (*30*), the authors have considered only one local region of ($\chi1$, $\chi2$) space for each of the tryptophans, including Trp^9.

DISCUSSION

The characteristics of gramicidin channels are determined largely by the aromatic tryptophans in the sequence. The aliphatic leucines next to the tryptophans are far from inert, however, as they modulate the effects of the Trp residues on channel folding and therefore help to regulate overall channel function (*13*). The conformational multiplicity in the triple-substituted gramicidins precluded a more detailed study of the side-chain/side-chain interactions in the (Trp-D-Leu)$_3$Trp segment.[2] In this study, therefore, we isolated the effect of a single D-Leu on a neighboring Trp and on global channel properties. In this discussion, we will consider the role of tryptophans in gramicidins, and the global and local influences of single versus triple aliphatic and aromatic substitutions near the tryptophans. Our overall conclusion will be that the gA indole rings are constrained to rather optimal local minima by the neighboring aliphatic D-Leu side chains with which they interact.

Tryptophans in Gramicidins. The linear gramicidins fold spontaneously into their functional channel conformation in membrane environments (or appropriate detergent micelles) (*44*, *45*)—but not in any known organic or aqueous solvents (*36*, *37*). Few systems have been examined both inside and outside of membranes, although the bilayer/solution interface is known to have an organizing effect on other peptides (*46*). It is therefore too early to ascertain whether this property of folding appropriately *only* within a membrane will be typical of membrane-spanning proteins, but such is a likely possibility. For the linear gramicidins, the need to arrange the tryptophans at the membrane/water interface drives the refolding from a solution double helix to a membrane-spanning channel (*3*, *4*, *6*, *8*, *47*−*49*). Gramicidins with reduced numbers of tryptophans (due to Trp → Phe substitutions) show reduced propensity for channel formation and greater tendency to remain double-helical within membranes (*2*, *4*−*8*). The structure-promoting effects of Trp, therefore, are most likely due to the ability of the indole NHs to from hydrogen bonds with H_2O and other polar groups at the interface (*3*, *4*).

In addition to driving the subunit folding, the gA tryptophans are important for ion transport through gramicidin channels. Though they do not directly contact the passing cations, the indole dipoles nevertheless promote both cation entry and cation flux through individual channels (*9*, *50*). Replacement of any one of the indoles by a simple phenyl ring reduces the single-channel conductance by ~20−30% (*8*). Conversely, enhancing one of the indole dipoles by 5-fluorination increases the single-channel conductance by ~20−30% (*10*) in a lipid-dependent manner (*11*).

Though critical for structure and function, the gramicidin tryptophans do not act alone. The Trps are spaced 2 residues

apart at positions 9, 11, 13, and 15 in the sequence, and the intervening D-leucines have important auxiliary roles to play.

Single versus Triple Substitutions. The effects of replacing only a single D-Leu (*in casu* D-Leu^{10}) can be compared to the effects of replacing the three D-leucines at 10, 12, and 14 of gA (*13*). As expected, the triple substitutions produce the more dramatic effects on structure. When positions 10, 12, and 14 are substituted with D-Ala or D-Val, the CD spectra and SEC chromatograms from the resulting gramicidins show at least 40% inert double-helical conformations in membranes (*13*), with even higher-order aggregates for [D-Ala^{10,12,14}]gA. By contrast, Figures 3 and 4 show that the single-stranded $\beta^{6.3}$ channel conformation is largely preserved when position 10 alone is substituted. Furthermore, the 8-fold reduction in average lifetime for [D-Ala^{10,12,14}]gA channels compared to only a 2-fold reduction for [D-Ala^{10}]gA channels relative to gA (Table 1)[6] may be considered a structural effect. Whereas we cannot exclude that D-Ala^{12} and D-Ala^{14} alter the folding and function of gramicidin to a greater extent than does D-Ala^{10}, we surmise that the effects of multiple Leu → Ala substitutions could be cooperative in terms of their effects on channel folding.

In terms of ion permeation, the single and triple D-Ala and D-Val substitutions produce similar reductions in cation conductance, relative to gA (Table 1). (It appears, therefore, that nearly all the reduction in g may be attributed to subsitutions at residue 10.) A single D-Phe^{10} substitution reduces g by nearly 50% (Table 1). Single-channel experiments following triple aromatic substitutions at 10, 12, and 14 are in progress (Providence, Koeppe, and Andersen, unpublished results).

It is interesting that the native gA sequence is nearly optimum for single-file, selective cation transport. Among hundreds of analogues that have been examined, only a straight aliphatic side chain or Ala at position one (*51*), a D-Ala at position 2 (*26*), and 5-fluorination of a Trp (*11*) have been found to increase the single-channel conductance, and the conductance change in the former two cases was only by about 10% over the conductance of channels formed by gA itself. The native gA single-channel lifetime is lipid dependent and intermediate (neither very slow nor very fast), being about 1 s in commonly used model membranes. The single-channel lifetime can easily be increased or decreased by changing the length or sequence of gA. Several strategies are available for increasing the channel lifetime, for example: improving the channel/membrane hydrophobic matching by lengthening the gA sequence (*52*), replacing the rather polar Gly^2 with D-Ala^2 (*26*), or interestingly, replacing all of the first five residues with the sequence Ala^1-D-Ala^2- Ala^3-D-Ala^4- Ala^5 (*53*). The natural design of gramicidin A—in terms of channel properties—therefore appears to favor nearly optimum cation conductance, complete rejection of anions, and intermediate channel lifetime.

Global Effects of Changing D-Leu^{10} Are Minimal. As noted above, gA retains its fundamental structural properties when residue 10 is changed to D-Ala, D-Val, or D-Phe. The new gramicidins are >90% single-stranded $\beta^{6.3}$ helices in DMPC, and the single-channel lifetimes remain 50−85% of the gA lifetime (Table 1). The retention of the same backbone conformation as gA is critical for interpreting the NMR spectra (see below). The largest decrease in single-channel conductance (Table 1) is seen for [D-Phe^{10}]gA and is probably a local effect of the phenyl ring, which also has a large effect on the NMR spectrum of d_5-Trp^9.

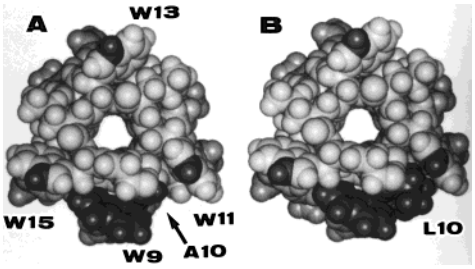

FIGURE 6: End view of space-filling molecular models for (A) [D-Ala10]gA and (B) native [D-Leu10]gA. The side chains of Trp^9 and residue 10 are shown dark, as are the indole NH groups of tryptophans 11, 13, and 15. Selected side chains are labeled using the one-letter amino acid code and residue number.

Local Effects on Trp^9 Are Small but Measurable. The first experimentally grounded model for the gA channel, in SDS, placed the indole ring of Trp^9 next to the side chain of D-Leu^{10} based on NOE interactions between the 9 and 10 side chains (*14, 20, 54*). Our data—both the acylation results (*19*) and the D-Leu^{10}-substitution results presented here—support this conformation for Trp^9 in DMPC also.

The first clue that Trp^9 should be near D-Leu^{10} in DMPC came from studies where the ethanolamine of gA was modified by acylation with palmitic acid. The palmitoyl chain passes between Trp^9 and D-Leu^{10} (*27*) and perturbs the ^{2}H NMR spectra of both residues 9 and 10 but, interestingly, has little effect on the spectrum of Trp^{11} (*19*). The conclusion that Trp^9 is near D-Leu^{10} is now further supported by the changes in the ^{2}H NMR spectra of Trp^9 when the identity of residue 10 is changed (Figure 5). These spectral changes correspond to changes of up to 7° in χ1 for Trp^9, and up to about 30° in χ2 (Table 2), for conservative substitutions at position 10.

The models in Figure 6 illustrate the packing of Trp^9 next to D-Leu^{10} in gA (Figure 6B), and next to the smaller side chain in [D-Ala^{10}]gA (Figure 6A). The overall effect is that the smaller D-Ala^{10} allows Trp^9 to assume approximately the same position and orientation that it has in the presence of D-Leu^{10} in native gA—a position that seems to be optimal, in the sense that the channel's ion permeability is nearly maximal (see above); but we admittedly do not understand why the conductance of [D-Ala^{10}]gA channels is less than that of gA channels. Furthermore, our fits to the NMR data suggest that the parameter m, which describes motional averaging of the Trp^9 ring, does not change with the smaller D-Ala^{10} side chain but remains about the same as in gA. D-Val^{10} or D-Phe^{10} causes steric crowding, and thereby "pushes" Trp^9 away from its preferred position. This creates a stress, which, rather than restricting the motion of the nearby ring, apparently causes the energy minimum for the Trp^9 ring to be less well defined on the NMR time scale. (A similar conclusion was reached for the NMR spectra from deuterated 5-F-Trp^9 and 6-F-Trp^9 in gA (*40*)). The uncertainty in the ring position is manifest as increased motional averaging in the NMR spectra. The perturbing D-Val^{10} and D-Phe^{10} side chains alter not only the average position but

[6] The single-channel results refer only to the $\beta^{6.3}$ channel conformation, because the double-helical conformations in question are nonconducting (*13*).

also the dynamics of the Trp[9] ring on the NMR time scale. In terms of function, the effect of D-Phe[10] is somewhat more conspicuous, since it reduces the single-channel conductance by nearly 50% (Table 1). It is noteworthy, nevertheless, that each of the position-10 substitutions preserves a channel structure and single-channel properties that are similar those of native gA. This feature has allowed local modulations near Trp[9] to be examined.

Conclusion. Conservative amino acid substitutions at D-Leu[10] of gramicidin A (gA) allow one to clarify the orientation of Trp[9] in gA channels and to characterize the aliphatic/aromatic "neighboring residue" effects on the structure as well as the function of gA channels.

REFERENCES

1. Sarges, R., and Witkop, B. (1965) *J. Am. Chem. Soc. 87*, 2011−2020.
2. Heitz, F., Spach, G., and Trudelle, Y. (1982) *Biophys. J. 40*, 87−89.
3. O'Connell, A. M., Koeppe, R. E., II, and Andersen, O. S. (1990) *Science 250*, 1256−1259.
4. Durkin, J. T., Providence, L. L., Koeppe, R. E., II, and Andersen, O. S. (1992) *Biophys. J. 62*, 145−159.
5. Salom, D., Bañó, M. C., Braco, L., and Abad, C. (1995) *Biochem. Biophys. Res. Commun. 209*, 466−473.
6. Cotten, M., Xu, F., and Cross, T. A. (1997) *Biophys. J. 73*, 614−623.
7. Salom, D., Pérez-payá, E., Pascal, J., and Abad, C. (1998) *Biochemistry 37*, 14279−14291.
8. Becker, M. D., Greathouse, D. V., Koeppe, R. E., II, and Andersen, O. S. (1991) *Biochemistry 30*, 8830−8839.
9. Fonseca, V., Daumas, P., Ranjalahy‗Rasoloarijao, L., Heitz, F., Lazaro, R., Trudelle, Y., and Andersen, O. S. (1992) *Biochemistry. 31*, 5340−5350.
10. Andersen, O. S., Greathouse, D. V., Providence, L. L., Becker, M. D., and Koeppe, R. E., II. (1998) *J. Am. Chem. Soc. 120*, 5142−5146.
11. Busath, D. D., Thulin, C. D., Hendershot, R. W., Phillips, L. R., Maughan, P., Cole, C. D., Bingham, N. C., Morrison, S., Baird, L. C., Hendershot, R. J., Cotten, M., & Cross, T. A. (1998) *Biophys J. 75*, 2830−2844.
12. Providence, L. L., Andersen, O. S., Greathouse, D. V., Koeppe, R. E., II, and Bittman, R. (1995) *Biochemistry 34*, 16404−16411.
13. Jude, A. R., Greathouse, D. V., Koeppe, R. E., II, Providence, L. L., and Andersen, O. S. (1999) *Biochemistry 38*, 1030−1039.
14. Arseniev, A. S., Lomize, A. L., Barsukov, I. L., and Bystrov, V. F. (1986) *Biol. Membr. 3*, 1077−1104.
15. Ketchem, R. R., Hu, W., and Cross, T. A. (1993) *Science 261*, 1457−1460.
16. Koeppe, R. E., II, and Andersen, O. S. (1996) *Annu. Rev. Biophys. Biomol. Struct. 25*, 231−258.
17. Koeppe, R. E., II, Killian, J. A., Greathouse, D. V., and Andersen, O. S. (1998) *Biol. Skr. Dan. Vid. Selsk. 49*, 93−98.
18. Hu, W., Lazo, N. D., and Cross, T. A. (1995) *Biochemistry 34*, 14138−14146.
19. Koeppe, R. E., II, Killian, J. A., Vogt, T. C. B., De‗Kruijff, B., Taylor, M. J., Mattice, G. L., and Greathouse, D. V. (1995) *Biochemistry 34*, 9299−9306.
20. Lomize, A. L., Orekhov, V. Y., and Arsen'ev, A. S. (1992) *Bioorg. Khimiya 18*, 182−200 (in Russian).
21. Hu, W., Lee, K. C., and Cross, T. A. (1993) *Biochemistry 32*, 7035−7047.
22. Koeppe, R. E., II, Killian, J. A., and Greathouse, D. V. (1994) *Biophys. J. 66*, 14−24.
23. Greathouse, D. V., Koeppe, R. E., II, Providence, L. L., Shobana, S., and Andersen, O. S. (1999) *Methods Enzymol. 294*, 525−550.
24. Greathouse, D. V., Hinton, J. F., Kim, K. S., and Koeppe, R. E., II (1994) *Biochemistry 33*, 4291−4299.
25. Andersen, O. S. (1983) *Biophys. J. 41*, 119−133.
26. Mattice, G. L., Koeppe, R. E., II, Providence, L. L., and Andersen, O. S. (1995) *Biochemistry 34*, 6827−6837.
27. Koeppe, R. E., II, Vogt, T. C. B., Greathouse, D. V., Killian, J. A., and De‗Kruijff, B. (1996) *Biochemistry 35*, 3641−3648.
28. Killian, J. A., Taylor, M. J., and Koeppe, R. E., II. (1992) *Biochemistry 31*, 11283−11290.
29. Gall, C. M., DiVerdi, J. A., and Opella, S. J. (1981) *J. Am. Chem. Soc. 103*, 5039−5043.
30. Ketchem, R. R., Roux, B., and Cross, T. A. (1997) *Structure 5*, 1655−1669.
31. Harada, Y., and Iitaka, Y. (1977) *Acta Crystallogr. B33*, 244−247.
32. Souhassou, M., Lecomte, C., Blessing, R. H., and Aubry, A. (1991) *Acta Crystallogr. B47*, 253−266.
33. Caminati, W., and Di‗Bernardo, S. (1990) *J. Mol. Struct. 240*, 253−262.
34. Slater, L., and Callis, P. (1995) *J. Phys. Chem. 99*, 8572−8581.
35. Serrano-Andres, L., and Roos, B. O. (1996) *J. Am. Chem. Soc. 118*, 185−195.
36. Wallace, B. A., Veatch, W. R., and Blout, E. R. (1981) *Biochemistry 20*, 5754−5760.
37. Killian, J. A., Prasad, K. U., Hains, D., and Urry, D. W. (1988) *Biochemistry 27*, 4848−4855.
38. LoGrasso, P. V., Moll, F. I., and Cross, T. A. (1988) *Biophys. J. 54*, 259−267.
39. Koeppe, R. E., II, Greathouse, D. V., Providence, L. L., and Andersen, O. S. (1999) In *Gramicidin and Related Ion Channel-Forming Peptides: Novartis Foundation Symposium 225* (Chadwick, D. J., and Cardew, G., Eds) pp 44−61, Wiley, Chichester.
40. Cotten, M., Tian, C., Busath, D. D., Shirts, R. B., and Cross, T. A. (1999) *Biochemistry 38*, 9185−9197.
41. Hing, A. W., Adams, S. P., Silbert, D. F., and Norberg, R. E. (1990) *Biochemistry 29*, 4144−4156.
42. Prosser, R. S., Davis, J. H., Dahlquist, F. W., and Lindorfer, M. A. (1991) *Biochemistry 30*, 4687−4696.
43. Prosser, R. S., Daleman, S. I., and Davis, J. H. (1994) *Biophys J. 66*, 1415−1428.
44. Andersen, O. S., Apell, H.-J., Bamberg, E., Busath, D. D., Koeppe, R. E., II, Sigworth, F. J., Szabo, G., Urry, D. W., and Woolley, A. (1999) *Nature Struct. Biol. 6*, 609.
45. Cross, T. A., Arseniev, A., Cornell, B. A., Davis, J. H., Killian, J. A., Koeppe, R. E., II, Nicholson, L. K., Separovic, F., and Wallace B. A. (1999) *Nature Struct. Biol. 6*, 610−611.
46. Kaiser, E. T., & Kézdy, F. J. (1983) *Proc. Natl. Acad. Sci. U.S.A. 80*, 1137−1143.
47. Bystrov, V. F., and Arseniev, A. S. (1988) *Tetrahedron 44*, 925−940.
48. Abdul-Manan, Z., and Hinton, J. F. (1994) *Biochemistry 33*, 6773−6783.
49. Arumugam, S., Pascal, S., North, C. L., Hu, W., Lee, K. C., Cotten, M., Ketchem, R. R., Xu, M., Brenneman, M., Kovacs, F., Tian, F., Wang, A., Huo, S., and Cross, T. A. (1996) *Proc. Natl. Acad. Sci. U.S.A. 93*, 5872−5876.
50. Becker, M. D., Koeppe, R. E., II, and Andersen, O. S. (1992) *Biophys J. 62*, 25−27.
51. Russell, E. W. B., Weiss, L. B., Navetta, F. I., Koeppe, R. E., II, and Andersen, O. S. (1986) *Biophys. J. 49*, 673−686.
52. Durkin, J. T., Providence, L. L., Koeppe, R. E., II, and Andersen, O. S. (1993) *J. Mol. Biol. 231*, 1102−1121.
53. Koeppe, R. E., II, Greathouse, D. V., Jude, A., Saberwal, G., Providence, L. L., and Andersen, O. S. (1994) *J. Biol. Chem. 269*, 12567−12576.
54. Arseniev, A. S., Barsukov, I. L., Bystrov, V. F., Lomize, A. L., and Ovchinnikov, Yu. A. (1985) *FEBS Lett. 186*, 168−174.
55. Bañó, M. C., Braco, L., and Abad, C. (1988) *J. Chromatogr. 458*, 105−116.

BI9920679